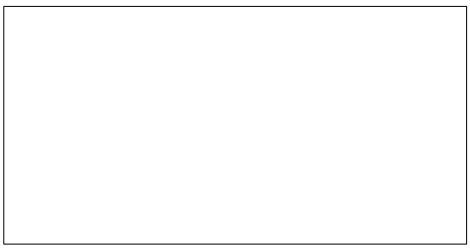

Amadi, Emmanuel Eni, Najafzadeh, Mojgan, Jacob, Badie K, Baumgartner, Adi ORCID logoORCID: https://orcid.org/0000-0001-7042-0308 and Anderson, Diana (2025) IN VITRO EVALUATION OF CYTOGENETIC DAMAGE BY GRAPHENE OXIDE (15-20 SHEETS) NANOMATERIALS IN HUMAN BLOOD LEUKOCYTES FROM HEALTHY INDIVIDUALS AND PULMONARY DISEASE PATIENTS DIAGNOSED WITH ASTHMA, COPD AND LUNG CANCER. International Journal of Engineering Technology Research & Management, 9 (8). pp. 98-124.

Downloaded from: https://ray.yorksj.ac.uk/id/eprint/12809/

The version presented here may differ from the published version or version of record. If you intend to cite from the work you are advised to consult the publisher's version: http://ijetrm.com/

Research at York St John (RaY) is an institutional repository. It supports the principles of open access by making the research outputs of the University available in digital form. Copyright of the items stored in RaY reside with the authors and/or other copyright owners. Users may access full text items free of charge, and may download a copy for private study or non-commercial research. For further reuse terms, see licence terms governing individual outputs. Institutional Repositories Policy Statement

RaY

Research at the University of York St John

For more information please contact RaY at ray@yorksj.ac.uk

iJETRM
International Journal of Engineering Technology Research & Management
(IJETRM)
https://ijetrm.com/

IN VITRO EVALUATION OF CYTOGENETIC DAMAGE BY GRAPHENE OXIDE (15-20 SHEETS) NANOMATERIALS IN HUMAN BLOOD LEUKOCYTES FROM HEALTHY INDIVIDUALS AND PULMONARY DISEASE PATIENTS DIAGNOSED WITH ASTHMA, COPD AND LUNG CANCER

Emmanuel Eni Amadi[1], Mojgan Najafzadeh[1], Badie K Jacob[2,3], Adi Baumgartner[4], and Diana Anderson[1,]
[1]School of Chemistry and Bioscience, Faculty of Life Sciences, University of Bradford, BD7 1DP UK.
[2]Bradford Royal Infirmary, Bradford, BD9 6RJ, UK.
[3] St Luke's Hospital, Bradford, BD5 ONA, UK.
[4]School of Health Sciences, York St John University, York, YO31 7EX, UK.
***Author for Correspondence**:
Dr Emmanuel Eni Amadi, School of Chemistry and Bioscience, Faculty of Life Sciences, University of Bradford, Bradford, West Yorkshire, BD7 1DP, UK.
E-mail: info@amadiglobal.co.uk

ABSTRACT
For the past few decades, the use of graphene oxide (GO) nanomaterials (NMs) has increased exceedingly due to their biomedical applications in the drug delivery of anti-cancer drugs. Their unique physicochemical properties and good surface chemistry with unbound surface functional groups enable covalent bonding with organic molecules such as RNA and DNA, making GO NMs excellent candidates for drug delivery nanocarriers. Despite the increased use in biomedical applications, there are concerns about their genotoxicity. Only a few studies on GO NMs' impact on DNA have been published on humans, let alone on patients diagnosed with chronic pulmonary diseases. This study investigates for the first time the effects of commercial GO (15-20 sheets; 4-10% edge-oxidized; 1 mg/ml) *in vitro*, in particular the DNA damage but also other genotoxic endpoints in whole blood and peripheral blood leucocytes (PBL) from healthy individuals and patients diagnosed with chronic pulmonary diseases, i.e., asthma, chronic obstructive pulmonary disease (COPD), and lung cancer. After detailed characterization of commercial GO NMs, cytotoxicity studies were conducted using the dimethyl thiazolyl diphenyltetrazolium bromide (MTT) and neutral red uptake (NRU) assays. In contrast, genotoxicity (DNA damage and chromosome aberration parameters) was studied using alkaline Comet and cytokinesis-blocked micronucleus (CBMN) assays. Our results showed concentration-dependent increases in cytotoxicity, genotoxicity, and chromosome aberrations, with PBL from COPD and lung cancer patients being more sensitive to DNA damage compared with asthma patients and healthy control individuals. GO NMs may have promising roles in drug delivery applications when formulated to deliver drug payloads to cells for treating COPD or cancer cells. But the fact that cytotoxicity, genotoxicity, and chromosome instability parameters as biomarkers of cancer risk were increased in exposed cells from healthy individuals should be of concern regarding public health, especially in occupational exposures and in medical treatments when using GO NMs as drug delivery nano-carriers.

Keywords:
Graphene Oxide, human whole blood, human peripheral blood leukocytes, asthma, chronic obstructive pulmonary disease, lung cancer, MTT assay, Neutral Red Uptake Assay, Comet assay, and Micronucleus assay.

1. INTRODUCTION

The use of GO NMs has increased significantly due to their application as a drug delivery platform for the treatment of several chronic diseases. The properties which make GO unique compared to other nanomaterials are the two-dimensional planar structure, high surface area-to-volume ratio of 2,600 m^2/g (Liu et al. 2013; Wu et

iJETRM
International Journal of Engineering Technology Research & Management
(IJETRM)
https://ijetrm.com/

al. 2015), surface chemistry of 4-10% edge-oxidization, and heavily unbound, surface functional groups such as hydroxy -OH, carboxyl /ketone -C=O, epoxy/alkoxy -C-O, and aromatic -C=C groups (Wang et al. 2011b; Mohamadi and Hamidi 2017). Their unique surface chemistry enables covalent bonding with bio-compatible polymers such as chitosan, polyethylene glycol (PEG) (Wu et al. 2015), and organic molecules (e.g. proteins, RNA, DNA, and drugs) making GO NMs excellent nanocarriers for drug delivery (Rebuttini et al. 2015).

GO NMs have been used to deliver different therapeutic agents including proteins, small drug molecules, antibodies, and DNA (Parveen et al. 2012). The large specific surface area of a single layer of nano-graphene sheets (NGS) allows a significant number of drugs to be loaded into its structure (Sun et al. 2008). Zhao and colleagues recently demonstrated that modified graphene sheets accept a doxorubicin payload that is covalently bound to the surface and later released through the action of glutathione (Zhao et al. 2015). Research using xenograft tumour mouse models also showed that NGS had a high uptake into tumour cells (Yang et al. 2010). Several factors have been identified to influence the effectiveness of GO-based drug delivery systems, including the structural design, drug loading capacity, biocompatibility in blood, and the efficiency of drug release at the right tumour site (Wang et al. 2011a; Liu et al. 2013). To improve the specificity of nanocarriers, the surface of GO NMs can be conjugated with ligands such as transferrin receptors (TfR) (Daniels et al. 2006), folic acid (Nasongkla et al. 2004), and polyclonal antibodies specific to certain tumour cells (Dinauer et al. 2005).
In this study, we aimed to evaluate the DNA damage responses (cytotoxicity, genotoxicity, and chromosome instability parameters) after perturbation by GO NMs in human blood samples (whole blood and peripheral blood leukocytes) *in vitro*.

2. MATERIALS AND METHODS

2.1 Chemicals

Graphene Oxide 15-20 sheets, 14-10% edge-oxidized, 1 mg/ml dispersion in H_2O (Cat. no. 794341); *In vitro* Toxicology Assay Kit Neutral Red based (Cat. no. Tox-4); bovine serum albumin (BSA; CAS No. 9048-46-8); ethidium bromide (CAS no: 1239-45-8); hydrogen peroxide (30% w/w; CAS no. 7722-84-1); mitomycin C (CAS no: 50-07-7); dimethyl sulfoxide (DMSO; CAS no. 67-68-5); Rosewell Park Memorial Institute medium 1640 (RPMI-1640: Cat no. R8758); cytochalasin B (CAS no. 14930-96-2) were purchased from Sigma-Aldrich, UK. RPMI medium 1640 with GlutaMAX™ (Cat. no. 61870010), low melting point (LMP) agarose (Cat. no. 16520050), normal melting point (NMP) agarose (Cat. no. 17850), foetal bovine serum (FBS), phytohaemagglutinin (PHA) (Cat. no. 10576015); 3-(4,5-dimethylthiazol-2-yl)-2,5-diphenyltetrazolium bromide MTT; CAS no. 298-93-1; Cat. No. M6494) were purchased from Thermo Fisher Scientific, UK. All other chemicals were of analytical grade and were sourced locally.

2.3 Characterisation of Graphene Oxide Nanomaterials

Preparation of GO Suspension for Particle Size and Surface Charge Analysis

Four different working stock concentrations of GO (10, 20, 50, and 100 µg/ml) were prepared from the 1 mg/ml stock dispersion to a final volume of 1,000 µl using pure water. All working stock suspensions were sonicated (Sonics Vibra Cell, Sonics & Materials Inc., New Town, USA) for 5 min at 30 W immediately before use.

Dynamic Light Scattering (DLS) and Zeta Potential (ZP) Analysis

A small volume of each working stock suspension was diluted 1:100 with pure water. For DLS measurements, the diluted solutions were transferred into plastic cuvettes and particle size distribution was measured in triplicate and at room temperature (RT; 25°C) using a Zetasizer Nano-ZS (Malvern Instruments, UK; Model ZEN3600). For ZP measurements, the diluted samples were transferred into a clean Zeta cell, and the ZP readings were measured using the same Zetasizer Nano-ZS at 25°C for 16 runs each. Before each measurement, the suspensions were mixed by gentle agitation to ensure that the particles were well dispersed in the suspension.

Scanning Electron Microscope (SEM) Analysis

For the SEM analysis, the different working stock suspensions of GO NMs (10, 20, 50 and 100 µg/ml) were allowed to air-dry overnight prior to loading the SEM sample stub onto the sample stage. The stub was then tightened and positioned in place to obtain better image. The sample stage was then placed inside the sample chamber and the compartment closed and evacuated Using the SEM software. the operating voltage was set to

iJETRM
International Journal of Engineering Technology Research & Management
(IJETRM)
https://ijetrm.com/

20.0 kV and the two-dimensional (2-D) SEM images were analysed at 20K magnification (FEI Quanta 400, Cambridge, UK).

Transmission Electron Microscope (TEM) Analysis

A TEM was used to measure the size and aggregation characteristics of the dried GO NMs. Briefly, the different working stock suspensions of GO (10, 20, 50 and 100 µg/ml) were first filtered through carbon-coated copper TEM grids (300 mesh), followed by washing off excess particles from the grids by dipping them 50 x in pure water. The dried grids containing the particles were then evaluated using the TEM (JEM-2100, JEOL Ltd., Tokyo, Japan) at 20.0 kV with various magnifications (50x; 1,000x; and 2,500x) and three-dimensional (3-D) TEM micrographs were obtained.

2.4 Blood Sample Collection

After informed consent was obtained, blood samples were collected by a trained phlebotomist in 5-ml Vacuette® LH lithium heparin-coated tubes. Ethical approval had been given by the University of Bradford's Research Ethics Sub-Committee for human individuals (Reference No.: 0405/8). It was also reviewed by the Leeds East Research Ethics Committee (Reference No. 12/YH/0464) and the Research Support and Governance Office, Bradford Teaching Hospitals NHS Foundation (Reference No. DA1202). Patients with asthma, COPD, and lung cancer were recruited from Professor Badie K Jacob's clinic at Bradford Royal Infirmary and Dr Abid Aziz's Respiratory Consultant's clinic at St Luke's Hospital NHS Trust, Bradford, West Yorkshire, UK. Healthy individuals were recruited from the University of Bradford's student community and volunteers from Blackley, North Manchester, UK. Blood samples were used on the day of collection. Unused blood that remained on the day of collection was diluted with RMPI-1640 1:2 followed by the addition of 10% DMSO. The diluted blood samples were then divided into aliquots and stored in a deep freezer at -80°C. Only fresh blood samples were used in the cytotoxicity and genotoxicity assays. The demographic data of healthy individuals and patients who participated in the study are shown in **Tables 1-4.**

2.5 Isolation of Peripheral Blood Leukocytes

Peripheral blood leukocytes (PBL) from healthy individuals and patients (asthma, COPD, and lung cancer) were isolated from whole blood using the Lymphoprep™ density gradient centrifugation method with slight modifications (Böyum 1968; STEMCELL Technologies 2017). They were transferred into 50 ml Universal tubes prefilled with 10 ml of 0.9% NaCl and then centrifuged at 630 x g for 15 min at room temperature (RT). After discarding the supernatant leukocyte pellets were resuspended in 700 µl of RPMI-1640 medium and the cells were counted using a Neubauer haemocytometer. The cell concentration was calculated, and the final volume of the leukocyte suspension was adjusted for cell culture.

2.6 Cytotoxicity assays

2.6.1 MTT and Neutral Red Uptake Assays

Isolated PBL from different blood donor groups (see Tables 1-4, grey shaded rows), i.e. from healthy individuals (11/AM, 12/WJ and 13/AN), asthma patients (18/0809845, 19/PU and 20/TA), COPD patients (18/CX, 19/QC and 20/0290072) and lung cancer patients (198/ZA, 19/4360497856 and 20/0795624), were treated with GO concentrations of 0.1, 0.2, 0.5 and 1 µg/ml in cell culture medium supplemented with 15% heat-inactivated foetal bovine serum (FBS) followed by an overnight incubation (16-18 hours) at 37°C. Thereafter, the MTT or (3-(4,5-dimethylthiazol-2-yl)-2,5-diphenyltetrazolium bromide) tetrazolium reduction assay - a colorimetric assay which measures the metabolic activity of mitochondria in living cells (Mossman 1983b), and the Neutral Red Uptake assay - which measures the metabolic activity of lysosomes in living cells in the presence of chemicals agent (Sigma-Aldrich USA 2018) - were performed according to the manufacturers' recommended guidelines. Absorbances of the dyes were measured. which are proportional to the number of living cells, was then quantified in triplicate (n = 3) using a spectrophotometer (Multiscan™ FC Microplate reader).

2.7 Genotoxicity Assays

2.7.1 Comet Assay

Diluted whole blood (1:10 in RPMI 1640) was treated with GO concentrations of 0.1, 0.2, 0.5 and 1 µg/ml, respectively. The addition of GO suspension was limited to 1% of the treatment volume of 1 ml. For the negative control (NC), the RPMI-1640 medium alone was used while 100 µM hydrogen peroxide (H_2O_2) served as a

iJETRM
International Journal of Engineering Technology Research & Management
(IJETRM)
https://ijetrm.com/

positive control (PC); 100 µM H_2O_2 was used as a PC as it induced significant DNA damage with more than 75% of the cells surviving (Amadi 2019). Incubation was carried out in a cell culture incubator for 30 min at 37°C prior to the alkaline Comet assay (pH >13) which was performed as previously described (Tice et al. 2000; Karbaschi and Cooke 2014; Azqueta and Dusinska 2015; OECD 2016).

2.7.2 Cytokinesis-Blocked Micronucleus (CBMN) Assay

RPMI-1640 culture medium with stable glutamine (Life Technologies, UK) supplemented with 15% foetal bovine serum (FBS; VWR, UK) and 1% penicillin-streptomycin solution (VWR, UK) was equilibrated to 37°C and 5% CO_2 for 30 min. Cell cultures were set up under sterile conditions using 4.5 ml of the equilibrated basic medium, 130 µl of phytohemagglutinin (PHA) and 400 µl of whole blood. After gentle mixing, they were then incubated at 37°C and 5% CO_2 for 24 hours. After 24 h of incubation, cells were treated with 0.1, 0.2, 0.5 and 1 µg/ml GO NMs. The addition of GO suspension was limited to 1% of the treatment volume of 5 ml. For the NC and PC, RPMI-1640 and 0.4 µM mitomycin C were used. The CBMN assay was performed as previously described (Fenech 2007). The nuclear division index (NDI) per treatment concentration was determined by scoring a minimum of 1,000 cells that included mono-, bi- and multinucleated cells (MonoNC, BiNC and MultiNC). The BiNCs result from proliferating cells allowing karyokinesis but inhibiting cytokinesis; they show two nuclei surrounded by a cytoplasm (Gerashchenko 2017). Cytogenetic damage was evaluated in BiNC by determining the induced micronuclei (MNi), nuclear plasmatic bridges (NPB) and nuclear buds (BUD) per 1,000 BiNC. Additionally, micronuclei in MonoNC were recorded. Experiments for each treatment group (healthy, asthma, COPD, and lung cancer groups) were repeated five times (n=5).

2.8 Statistical analysis

The data were expressed as the mean ± SEM, and statistical analysis was performed using the GraphPad Prism® software, version 7.04 (Fay Avenue, La Jolla, CA, USA) with built-in One-Way ANOVA and Dunnett's post-hoc multiple comparison tests to determine differences in cytotoxicity, genotoxicity, and frequencies of cytogenetic parameters (MNi, MonoNC, BiNC, MultiNC, NPBs and NBUDs) in treated cells (healthy individuals and patients: asthma, COPD, and lung cancer) relative to the untreated, NC samples. Statistical significance was accepted at $p < 0.05$, with * $p < 0.05$; ** $p < 0.01$; *** $p < 0.001$; and ns = not significant.

3.0 RESULTS

3.1 Particle Size Distribution / Agglomeration State, and Surface Charge

In this study, we characterized GO NMs using the Zeta sizer Nano to determine the particle size-distribution and surface charge in an aqueous solution. The results regarding DLS (dynamic light scattering), TEM and SEM (transmission and scanning electron microscopy) are shown in **Table 5**. For the size-distribution, we observed that GO NMs were well dispersed after gentle shaking before the experiment, but gradually agglomerated on the base of the cuvette after some time. The average hydrodynamic size / Z-Average (d.nm) of GO agglomerates with 15-20 layers was 760±31 nm, i.e. the particle size of each layer was 38-51 nm thick; the polydispersity index (PdI) - which estimates the broadness of the particles was 0.87±0.05; while the mean electro-kinetic zeta potential (ZP) or surface charges was -23±2 mV. In aqueous dispersion, sheets of GO NMs agglomerated forming large flakes of GO sheets on top of each other due to high inter-particulate forces of attraction (Van der Waal forces).

SEM and TEM analyses showed that the particle distances (nm) of measured GO aggregates were much lower compared to DLS. Particle sizes of GO NMs (15-20 sheets) were determined to be between 364 ± 29 nm and 448 ± 60 nm, while the average size of each layer was between 18 and 30 nm. The 2-D and 3-D micrographs from SEM and TEM (**Figure 1**) showed multiple layers/aggregates of GO NMs, a confirmation that the GO NMs used in this study have many layers (15 to 20 sheets) as described by the manufacturer (Sigma-Aldrich). Specifically, the TEM micrographs showed massive lumps of GO sheets tightly clogged on top of each other in a high agglomeration state: aggregated small sheets of GO layered on top of larger agglomerates all competing for space.

3.2 Cytotoxicity and Viability

3.2.1 NRU (Neutral Red Uptake) and MTT assays

iJETRM
International Journal of Engineering Technology Research & Management
(IJETRM)
https://ijetrm.com/

The percentage (%) of cell survival in the NRU and MTT assays was plotted against different concentrations of GO NMs (**Figure 2**). A close observation of the two graphs showed that at lower concentrations of up to 0.2 µg/ml, GONPs were cytotoxic as demonstrated by sharp slopes, while higher concentrations from 0.2 to 1.0 µg/ml showed high cytotoxicity to PBL as demonstrated by the continuous decreases of the slopes in each treatment group - healthy individuals (black colour), asthma (blue colour), COPD (green colour), and lung cancer (red colour).

In the NRU assay (**Figure 2A**), the % cell survival rates of PBL after treatment with 0.1 µg/ml (healthy individuals) decreased in a non-significant manner from 100% to 93.6%. However, for asthma, COPD and lung cancer groups, the % cell survival rates decreased very sharply in a statistically significant manner to 67.29% (asthma group, $p < 0.01$) to 65.6% (COPD group, $p < 0.05$) and the lowest value of just under 60% (lung cancer group, $p < 0.01$). On the other hand, as the GO concentrations increased from 0.1 to 0.2 µg/ml, the % cell survival rates of PBL from healthy individuals decreased sharply to 70.71% ($p < 0.01$), while cells from patient groups showed gradual significant decreases in % cell survival rates to 61.14% (asthma group, $p < 0.001$); 57.01% (COPD group, $p < 0.001$) and to 49.48% (lung cancer group, $p < 0.01$). After exposure to 0.5 and 1 µg/ml GO, the % cell survival rates of PBL decreased gradually in a significant manner ($p < 0.01$) as shown in the slopes of the gradients to 69.96% and 51.21% in the healthy individual group, to 57.24% and 55.57% in the asthma group, to 46.69 and 38.60% in the COPD group and 39.35% and 27.74% in the lung cancer group, respectively. Overall, the % cell survival rates of leukocytes from lung cancer patients were the lowest compared to COPD, asthma, and healthy controls.

In the MTT assay (**Figure 2B**), the % cell survival rates of PBL decreased after treatment with different concentrations of GO NMs (0.1, 0.2, 0.5, and 1 µg/ml). Specifically, after treatment with GO NMs between 0.1 and 0.2 µg/ml, the % cell survival rates significantly decreased ($p < 0.01$) in a concentration-dependent manner from 100% to 83.08% and 55.01% in the Healthy Individual Group, to 80.01 % and 61.67% in the asthma group, to 74.99% and 50.03% in the COPD group and 70.01% and 43.46% in the lung cancer group, respectively. When PBL were treated with higher concentrations of GO NMs 0.5 and 1 µg/ml, the % cell survival rates significantly decreased further($p < 0.001$) to 41.99% and 35.02% (Healthy Individual Group), to 44.97% and 40.04% (asthma group), 34.99% and 26.99% (COPD group) and to the lowest values of 29.99% and 20.60% (lung cancer group), respectively.
Overall, the % cell survival rates of leukocytes from lung cancer patients in both NRU and MTT assays were the lowest ($p < 0.001$) when compared to the other treatment groups (COPD, asthma, and healthy controls).

3.3 Genotoxicity and DNA Damage
3.3.1 The Comet Assay

The findings of the Comet assay are presented for both parameters, OTM and % tail DNA, in the histograms shown in **Figure 3A** (OTM) and **Figure 3B** (% tail DNA). GO NMs caused significant DNA damage to PBL in a concentration-dependent manner (0.1, 0.2, 0.5 and 1 µg/ml) after 30 min of exposure when compared to untreated cells. For each GO concentration, PBL that originated from lung cancer patients (lung cancer group) showed the highest level of induced DNA damage for both parameters, OTM and % tail DNA, followed by the COPD group and the asthma group. PBL from healthy individuals (control group) showed the lowest levels of DNA damage. Notably even for the lowest concentration of 0.1 µg/ml, DNA damage (% tail DNA) in PBL was found to be significantly ($p < 0.001$) higher for the lung cancer group, followed by the asthma and COPD groups. A closer observation of the untreated PBL of the negative control showed basal DNA damage for all groups; however, significantly more for the lung cancer group ($p < 0.001$) followed by the COPD group ($p < 0.01$) when compared to the healthy control group. The baseline DNA damage in PBL of both healthy individuals and asthma patients showed no significant difference.

3.3.1 The CBMN assay

For the CBMN assay, whole blood was used for cultures, lymphocytes were stimulated to proliferate and then treated with 0.1, 0.2, 0.5 and 1 µg/ml GO NMs. The blood originated from healthy individuals (control group) but also from asthma, COPD, and lung cancer patients (asthma, COPD, and lung cancer group). The frequencies of

iJETRM
International Journal of Engineering Technology Research & Management
(IJETRM)
https://ijetrm.com/

seven biomarkers for cytogenetic damage, i.e., mono-, bi- and multinucleated cells (MonoNC, BiNC & MultiNC), nucleoplasmic bridges (NPB), nuclear buds in BiNC (BiNBUD), the nuclear division index (NDI) and the frequency of micronuclei in BiNC (BiMNi) were scored; **Table 6** shows findings for healthy individuals of the control group, the asthma group, the COPD Group, and the lung cancer group, respectively.

Mononucleated cells: For the control group, the percentage of MonoNC decreased significantly ($p < 0.001$) in a concentration-dependent manner from 38.12 ± 1.10% for the lowest concentration of 0.1 µg/ml to 24.52 ± 0.63% for the highest GO concentration of 1 µg/ml. This significant decrease ($p < 0.001$) was also seen for the three patient groups: from 35.20 ± 0.81% to 25.16 ± 0.79% (asthma group), from 33.12 ± 0.55% to 21.52 ± 0.55% (COPD group) and from 32.24 ± 1.80% to 15.56 ± 1.31% (lung cancer group), respectively. Therefore, the induction of MonoNC was the lowest in cancer patients, followed by COPD and asthma patients when compared to the healthy control group.

Binucleated cells: After treatment with GO NMs, a concentration-dependent significant increase of BiNC ($p < 0.001$) was observed. Specifically, for the control group of healthy individuals the percentage of BiNC (%BiNC) significantly increased from 61.16 ± 1.11% for the lowest concentration to 73.52 ± 0.26% for the highest GO concentration, respectively. For the three patient groups, the same pattern of significant increase was seen ($p < 0.001$): from 63.84 ± 0.88% to 72.24 ± 0.72% (asthma group), from 65.72 ± 0.52% to 75.84 ± 0.66% (COPD group) and from 66.16 ± 1.64% to 80.04 ± 1.26% (lung cancer group), respectively. The induction of BiNC was highest in the PBL from lung cancer patients followed by those from COPD and asthma patients when compared to the healthy negative control.

Multinucleated cells: polynuclear cells with three or four nuclei per cell (Ben-Ze'ev and Raz 1981) were assessed after exposure of PBL to GO NMs and the frequency of these induced MultiNC was recorded. For the healthy negative control, the percentage of MultiNC (%MultiNC) significantly increased ($p < 0.001$) with increasing GO concentrations from 1.44 ± 0.21% for the lowest concentration to 4.47 ± 0.41% for the highest concentration. For the asthma group significant numbers of MultiNC were induced from concentrations higher than 0.2 µg/ml. %MultiNC from 1.92 ± 0.27% to 5.20 ± 0.44% were observed. For the COPD group, the lowest concentration of 0.1 µg/ml significantly increased ($p < 0.001$) the percentage of MultiNC from 2.32 ± 0.15% to 2.64 ± 0.16% while doubling the concentration to 0.2 µg/ml resulted in a significant decrease to 2.16 ± 0.10% ($p < 0.001$) possibly due to aggregation of GO particles. Then up to 1 µg/ml, the proportions of %MultiNC increased significantly ($p < 0.001$) to 4.40 ± 0.31% and 5.28 ± 0.74%, respectively. For the lung cancer group, a significant increase was seen ($p < 0.001$) at concentrations higher than 0.2 µg/ml from 3.20 ± 0.42% to 8.80±0.68%, respectively. In summary, the highest induction of MultiNC was observed in the lung cancer group followed by the COPD and asthma groups when compared to the healthy negative control.

Nuclear division index (NDI): The NDI was calculated using the following Michael Fenck's method using the following formula:

$$NDI = \frac{M1 + 2M2 + 3M3}{N}$$

Where M1 = MonoNC; M2 = BiNC; M3 = MultiNC which includes tri- and tetranucleated cells, and N = the total number of viable cells scored (1,000) per concentration (Heshmati et al. 2018). The NDI is an indicator of cytostatic events and a biomarker of cell proliferation and mitogenic response in the presence of cytotoxic agents (Ionescu et al. 2011). The NDI values increased significantly ($p < 0.001$) with increasing GO concentrations (0.1, 0.2, 0.5 and 1 µg/ml) in the healthy control group from 1.63 ± 0.01 to 1.79 ± 0.00 for the highest dose. For the asthma group, the NDI increased significantly ($p < 0.001$) from 1.66 ± 0.01 to 1.77 ± 0.01 for the highest dose. Slight fluctuations might be attributed to GO NMs forming aggregates during incubation because there was no agitation during the time of incubation. For the COPD group, significant increases were seen in concentrations of 2 µg/ml and above from 1.69 ± 0.01 to 1.81 ± 0.01. The results for the lung cancer group were like those of the COPD group. A significant increase ($p < 0.001$) was observed for all concentration points from 1.69 ± 0.02 to 1.89 ± 0.01 for the highest concentration.

iJETRM
International Journal of Engineering Technology Research & Management
(IJETRM)
https://ijetrm.com/

Frequencies of induced MNi: The number of induced MNi and other cytogenetic parameters have been used as biomarkers (**Table 6**) of genome instability leading to the progression of certain cancer types such as urethral carcinoma (Podrimaj-Bytyqi et al. 2018). The mean frequencies of induced MNi were observed as micronuclei per 1,000 scored binucleated cells (BiMNi) or mononucleated cells (MonoMNi). In the healthy control group, a significant decrease of induced BiMNi from 1.80 ± 0.66 to 0.80 ± 0.37 and 1.00 ± 0.32 was observed after treatment with 0.1 and 0.2 µg/ml of GO, respectively ($p < 0.001$). The values peaked again at concentrations of 0.5 and 1 µg/ml at 3.00 ± 0.71 and 2.80 ± 0.66. For the asthma group, the number of induced MNi at concentrations of 0.1 and 0.2 µg/ml of GO decreased significantly ($p < 0.001$) from 2.40 ± 0.98 to 1.80 ± 0.66 per 1,000 BiNC, respectively. However, after exposure to 0.5 and 10 µg/ml of GO, the mean values of induced BiMNi increased significantly ($p < 0.001$) to 5.20 ± 0.80 and 5.80 ± 1.24, respectively. For the COPD group, PBL treated with 0.1 µg/ml of GO resulted in a decrease in BiMNi induction from 3.80 ± 80 to 3.20±0.58 ($p < 0.001$). However, upon treatments with 0.2, 0.5 and 1 µg/ml, more BiMNi were significantly induced ($p < 0.001$) resulting in frequencies of 5.60 ± 1.03, 5.80 ± 1.46 and 6.00 ± 0.45 per 1,000 BiNC, respectively. For the lung cancer group, all doses of GO NMs caused significant ($p < 0.001$) concentration-dependent increases in induced BiMNi: from 3.40 ± 0.51 to 9.40 ± 0.51 for the highest dose.

Chromosome Instability Parameters (NPBs, NBUDs, and MonoMNi)

Chromosomal instability parameters such as nucleoplasmic bridges (NPBs) and nuclear buds (NBUDs) as well as MonoMNi frequencies are used to assess different types of induced cytogenetic damage and were scored in the CBMN assay (**Table 6**). They are some of the biomarkers of cancer progression and are applied in both cancer diagnosis, prognosis, and pharmacotherapeutic outcomes (Vargas-Rondon et al. 2018).

Healthy control group: After treatment with 0.1, 0.2 and 1 µg/ml a small induction of NPBs in binucleated cells (BiNPBs) were observed; for the highest concentration a significant induction of BiNPBs ($p < 0.001$) was observed at 0.60 ± 0.24 per 1,000 BiNC. The highest concentration of GO also significantly induced ($p < 0.001$) BUDs in binucleated cells (BiNBUDs) at a frequency of 0.40 ± 0.24 per 1,000 BiNC. With increasing GO concentrations an increasing number of MNi in mononucleated cells (MonoMNi) were observed. At the highest concentration of 1 µg/ml the frequency of MonoMNi significantly increased ($p < 0.001$) from 0.40 ± 0.24 to 2.60 ± 0.93 per 1,000 MonoNC (extrapolated from raw numbers).

Asthma group: PBL treated with 0.1 µg/ml of GO did not induce BiNPBs, but treatment concentrations of 0.2, 0.5 and 1µg/ml significantly induced ($p < 0.001$) NPBs in BiNC. The highest concentration of GO resulted in 1.20 ± 0.58 per 1,000 BiNC. The highest concentration also resulted in a significant increase ($p < 0.001$) in BiNBUDs from 0.40 ± 0.24 to 1.40 ± 0.60 per 1,000 BiNC. The frequencies of the MonoMNi were also induced significantly ($p < 0.001$) after treatment with 0.1, 0.2, 0.5 and 1 µg/ml of GO NMs from 1.00 ± 0.32 to 5.20 ± 0.97 per 1,000 MonoNC (extrapolated).

COPD group: Exposed PBL of COPD patients showed as well only minimal induction of BiNPBs. At the highest concentration of GO, 0.60 ± 0.24 per 1,000 BiNC were significantly induced ($p < 0.001$). An induction of BiNBUDs as well as MonoMNi was observed in exposed PBL: for the highest concentration of GO a significant induction ($p < 0.001$) to 1.40 ± 0.40 per 1,000 BiNC and 3.20 ± 1.11 per 1,000 MonoNC (extrapolated) was seen, respectively.

Lung cancer group: The number of BiNPBs found in untreated PBL was 2.00 ± 0.63 per 1,000 BiNC. However, PBL exposed to GO (0.1, 0.2, 0.5 and 1 µg/ml) showed significantly lower ($p < 0.001$) numbers of BiNPB from 0.20 ± 0.20 to 1.00 ± 0.45, respectively. BiBUDs were also significantly induced ($p < 0.001$) to 1.00 ± 0.32 for the highest GO dose; the negative control did not show any BiBUDs. MNi in 1,000 extrapolated mononucleated cells were significantly induced ($p < 0.001$): from untreated control levels 2.80 ± 0.66 to 7.40 ± 0.51 for the highest GO concentration of 1 µg/ml.

3.5 Confounding Factors

A total of 80 individuals were randomly selected for blood donation to participate in the study, 55 % were males and 45 % were females (**Table 7**). In healthy individuals, age and absent cigarette smoking history were not considered confounding factors: 95% were under the age of 60 years, and 100% of participants had no smoking history. However, for patients in the asthma group, confounding factors of cigarette smoking and age might have impacted the results: 25% had a history of cigarette smoking and 65% were under 60 years of age. For patients in the COPD group, 100% of participants had a history of smoking and 65% were under the age of 60. For patients

iJETRM
International Journal of Engineering Technology Research & Management
(IJETRM)
https://ijetrm.com/

in the lung cancer group, there were confounding effects due to cigarette smoking (90%) and age (30% under 60 years of age).

4. DISCUSSION

Because of the increasing use of nanoparticles, it is vital to characterise them *in vitro* to ascertain their physical properties such as lateral size, surface charge, etc. The toxicity of nanomaterials such as graphene oxide has been linked to their physicochemical properties (Ou et al. 2016). The particle size measurements using DLS size distribution resulted in higher mean values than those obtained from microscopic analyses (SEM and TEM). One of the reasons could be linked to the physical condition of the nanomaterials during measurements. The DLS measures the Brownian motions of particles suspended within a liquid (aqueous dispersion) at a given temperature (Stetefeld et al. 2016). In an aqueous dispersion, water molecules are inserted into the GO interstitial spaces giving rise to false big particle sizes compared to SEM and TEM analyses performed with dried particles (Song et al. 2014).

The Zeta potential (ZP) analysis measures the electrostatic surface charge (Clogston and Patri 2011) of particulate matter in solution or colloids using the Zetasizer Nano ZS (Malvern instruments, UK). It offers quantitative data about the stability of nanoparticles in a given dispersion medium as well as the possibility of nanomaterials entering the cells through the cell membrane (Clogston and Patri 2011). The negative Zeta potential (ZP) value (-23 ± 2 mV) obtained in our study showed that GO NMs have a net-negative surface charge due to the nature of their surface chemistry: unbound hydroxy -OH, carboxyl/ketone C=O, epoxy/alkoxy C-O, and aromatic group C=C groups (Song et al. 2014).

Research has shown that the surface chemistry of GO NMs ($C_{14}H_{42}O_{20}$) tends to cause aggregation on the graphene plane (Yan and Chou 2010). GO NMs are amphiphilic, and thus possess both hydrophilic (polar) and lipophilic (non-polar) properties in aqueous dispersion (Kim et al. 2012). The negative ZP of around -23 mV that was measured was low, but the inter-particulate forces of attractions (Van der Waals forces) were high enough to cause GO NMs to agglomerate. Thus, the higher the ZP value, either positive or negative, the more stable is the dispersion. Since our values were close to ±30 mV, the GO NMs used in the study were considered to be stable in aqueous dispersion (Mittal et al. 2017).

Although size measurement with DLS has been widely applied in nanoparticle characterization, especially for monodispersed materials, the DLS technique might be less reliable for highly poly-dispersed NMs and thus might be unsuitable for size measurements of GO NMs with 15-20 sheets. It has been shown that the intensity of the light scattered by smaller particles in the dispersion medium might be swiftly covered by light intensities from bigger particles even if the bigger particles are very minute (Powers et al. 2006; Filipe et al. 2010; Bhattacharjee 2016). A second limitation of the DLS is its inability to discriminate particles based on their composition (Hondow et al. 2012). For instance, Hondow and colleagues reported that DLS failed to analyse nanoparticle size in the presence of serum proteins as they were forming protein corona, i.e., serum protein-to-particle binding occurred (Hondow et al. 2012; Barbero et al. 2017). This effect modified particle size and scattered light with higher intensity, which was then recorded as a larger particle size leading to false-positive results.

To address some of the limitations encountered using the DLS technique, also alternative techniques such as SEM and TEM were used. TEM has a higher resolution than SEM because an electron beam with shorter wavelengths was used (Winey et al. 2014). Regardless of any advantages in TEM analysis, several limitations were noted elsewhere (Winey et al. 2014). TEM can only analyse one sample at a time, termed drop-cast TEM, where samples dispersed in a medium are dropped and allowed to air-dry on a copper grid before imaging. Although the particle sizes, shape and sample composition can be analysed with TEM, this technique may not be a reliable method to measure particle agglomeration because the particles tend to agglomerate as the liquid components evaporate (Hondow et al. 2012; Wills et al. 2017). Moreover, the intensity of the electron beam could damage the samples during analysis, and as such TEM may not be a suitable method for thermolabile samples. Another key limitation of nanoparticle characterization using TEM is that the micrographs produced are cross-sectional 2-D images of agglomerated particles with several images observed at various points during the analysis which are eventually 3-D images (Wills et al. 2017).

iJETRM
International Journal of Engineering Technology Research & Management
(IJETRM)
https://ijetrm.com/

To overcome some of the above limitations found in DLS, SEM, and TEM, the use of alternative methods such as digital Fourier microscopy (DFM), cryogenic plunge freezing, etc. has been suggested elsewhere (Wills et al. 2017). The cryogenic freezing technique involves snap-freezing of a nanoparticle-suspension in liquid nitrogen or liquid ethane, freezing the liquid components and preserving them without distorting the integrity of the dispersed nanoparticles. This method is regarded as an excellent technique that can maintain the samples in their most natural form giving rise to stable samples adequate for imaging and particle size evaluation of thermolabile nanoparticles (Wills et al. 2017). Samples prepared in this way could be warmed under a high vacuum, which allows the liquid phase to sublime (change from solid to vapour) without affecting the integrity of the dispersed nanoparticles.

Assessment of the cell proliferation profile is a measure of cell viability - determining the cells' metabolic profile or survival in the presence of toxic chemicals. Their toxicity to cells may be a result of various mechanisms including physical destruction of the cell membranes, permanent binding of particles to protein receptors and total inhibition of protein synthesis (Aslantürk 2017). To evaluate cell death induced by toxic agents, it is vital to select robust and well-established cytotoxicity assays which are cheap, reproducible, and capable of producing reliable results. Before choosing the MTT and NRU assays in this study, several factors had to be considered, including sensitivity, reliability, and complexity of the protocol. It was their sensitivity and reliability parameters which stood out. The MTT and NRU assays are colorimetric assays commonly used to assess cytotoxicity or cell viability (Mossman 1983a) by evaluating the activities of mitochondrial enzymes and lysozymes, respectively (Stone et al. 2009). Due to their reliability and sensitivity, they are widely used in industries for drug screening (Hansen and Bross 2010). However, the NRU assay is cheaper, more sensitive, and less time-consuming compared to the MTT assay (Repetto et al. 2008). Between 0.1 and 0.2 µg/ml, GO NMs showed genotoxicity in the absence of cytotoxicity with no artefacts in both NRU and MTT assays, while treatment with higher concentrations up to 1 µg/ml caused irreversible cytotoxicity.

Human cell lines treated with GO NMs *in vitro* may not be the ideal tool for different types of biological research as these cell lines may contain mutations and chromosomal aberrations that could have arisen after several cell divisions. Consequently, the toxicity reports of cell lines may not expansively replicate the actual effects of GO NMs *in vivo* when tested on human lymphocytes and whole blood (Ding et al. 2014). Previous research on GO NMs (1-2 layers) exposed blood cells showed conflicting results. For instance, Sasidharan and colleagues showed that GO concentrations up to 75 µg/ml had little or insignificant haemolytic effects on blood cells (Sasidharan et al. 2012), but the work by Liao and colleagues was contradictory and demonstrated that GO had concentration-dependent haemolytic effects on blood cells (Liao et al. 2011). Haemolytic activity of GO NMs was also observed; exposure concentrations as low as 2 µg/ml had thrombo-toxic effects on platelets (Singh et al. 2011). However, in a follow-up study modified graphene, i.e., graphene amine (G-NH_2), did not cause thrombo-toxic effects (Singh et al. 2012). Some of these apparent contradictions might be associated with the physicochemical surface properties of a GO-like surface morphology; but also with the composition in the GO batch, i.e., artefacts or impurities, might play a role depending on the method through which GO was synthesized (Liao et al. 2011). To allow for consistency throughout our study, commercial graphene oxide was used. Although the MTT and NRU assay results demonstrated a general decrease in cell proliferation or an increase in cytotoxicity with increased concentrations, both assays did not follow the same trend. This deviation could be attributed to the reaction between the MTT dye and GO (Liao et al. 2011).

No matter how robust the MTT and NRU assays are, numerous studies have shown that the components of the reagents can interact with carbon NMs resulting in either inflated viability or false positive responses (Monteiro-Riviere and Inman 2006). For instance, carbon-based nanomaterials such as GO can reduce the MTT reagent, resulting in an overestimation of cell viability or could potentially mask cytotoxic responses (Monteiro-Riviere and Inman 2006).

GO prepared with the chemical exfoliation method (Hummer's method) contains significant amounts of catalytic ions such as manganese (Mn^{2+}) and ferrous ions (Fe^{2+}) (Liu et al. 2013). The presence of such impurities may result in unusually high levels of cytotoxicity, genotoxicity, and random scission of DNA, indicating the

iJETRM
International Journal of Engineering Technology Research & Management
(IJETRM)
https://ijetrm.com/

importance of purification of GO NMs before use as it could lead to false-positive results. Research shows that organic pollutants such as Mn^{2+} impurities on carbon nanotubes induced significant biological effects (Stéfani et al. 2011). Exposure of human neuroblastoma cells (SH-SY5Y) to Mn^{2+} decreased cell viability in a concentration-dependent manner (Stephenson et al. 2013).

The MTT assay could fail to accurately predict GO toxicity due to the spontaneous reduction resulting in a false positive GO autofluorescence signal (Wu et al. 2015; Ou et al. 2016). One of the suggested alternative methods is the water-soluble tetrazolium salt reagent (WST-8 assay) to establish that the viability results obtained from the assays were free of any interference /artefacts that might be induced by the GO nanomaterial itself. The viability of the cells at the time of treatments with MTT and NRU dyes should also be considered as a factor that might lead to false positive results. It has been reported that in the presence of GO NMs the viability of T lymphocytes is significantly reduced after 24 hours, depending on the concentration (Ding et al. 2014). Since the MTT and NRU dye solutions were treated after 24 h of lymphocyte treatment and incubation, and then further incubated for an additional 4 and 3 h respectively, it is likely that cell death (apoptosis or necrosis) might have occurred naturally even before the assay was completed.

Confounding factors may have also played important roles in the significant cytotoxicity responses observed in both COPD and lung cancer patients since 100% of individuals with COPD and lung cancer were smokers, with some of them smoking up to 30 cigarettes per day.

From the Comet assay results, it was evident that DNA damage increased significantly with increasing GO concentrations, but also depending on the pathological conditions of the individuals who participated in the study. However, this pattern might not always hold as true since increased concentrations might lead to particle agglomeration and subsequently lead to less particle contact with the cells. Especially in cells from patients with chronic pulmonary diseases (asthma, COPD, and lung cancer), it was generally observed that lymphocytes that were collected from lung cancer patients had the most significant DNA damage than those from COPD patients relative to observed DNA damage in cells from healthy control individuals, treated or untreated (NC). Increased DNA damage in lung cancer patients is attributed to the fact that lung cancer patients have less capacity to repair damaged DNA, leading to genetic changes (mutations) and progression to lung cancer (Orlow et al. 2015). In other words, their DNA is more vulnerable to genotoxic particles. Lymphocytes from patients with asthma and healthy individuals showed almost the same level of DNA damage. A study by Stephenson and colleagues demonstrated that Mn^{2+} and Fe^{2+} caused DNA damage in cells when assayed by the alkaline Comet assay (Stephenson et al. 2013). It is, therefore, imperative to assess the presence of impurities in GO, especially commercially purchased GO and if possible, to quantify their levels before comprehensive cytotoxicity and genotoxicity studies could be established.

The CBMN assay was used to evaluate cytogenetic damage and chromosome instabilities of cells which have completed one nuclear division. The inhibition of cytokinesis (a division of the cytoplasm) at the end of mitosis (nuclear division) by cytochalasin B resulted in binucleated cells (BiNC); cells that do not divide, e.g., because of the exposure to GO, were still visible as mononucleated cells (MonoNC). Chromosomal fragments which failed to segregate with the mitotic spindle were evaluated in BiNC but also MonoNC (Kirsch-Volders and Fenech 2001; Fenech 2002). Accumulation of the cytogenetic damage markers such as the frequency of MNi are hallmarks of lung cancer (El-Zein et al. 2008) depending on the pathological state of the individuals.

Our results highlight the implications of the genotoxicity of GO NMs (15-20 sheets) and the necessity for further research. On one hand, significantly higher levels of CBMN endpoints were observed in lymphocytes from both cancer and COPD groups, which is a good demonstration that GONPs could be an excellent candidate in drug delivery of anti-cancer drugs (Ma et al. 2015) and GO could be used for nanotherapeutics treating COPD (Seshadri and Ramamurthi 2018). The induction of MNi, a biomarker for cytogenetic damage, was significantly higher in lymphocytes that originated from lung cancer patients ($n = 5$; $p < 0.001$) followed by those from COPD patients. MNi are chromatin-containing bodies representing chromosomal fragments or even whole missegregation (Albertini et al. 2000). Therefore, GO could be classified as both a clastogen causing chromosomal breaks when directly or indirectly interacting with DNA – and an aneugen leading to missegregated chromosomes when

iJETRM
International Journal of Engineering Technology Research & Management
(IJETRM)
https://ijetrm.com/

interfering with the spindle apparatus during mitosis (Bignold 2009). GO's ability to induce DNA DSBs results in chromosomal fragments that are missegregation during the anaphase of mitoses. This leads to the formation of MNi being visible in the CBMN assay. Addition of cytochalasin B at 44 hours after the start of the blood culture (20 hours after treatments with GO and MMC) stopped cytokinesis after the formation of the daughter nuclei.

The implication of significant induction of cytostatic event parameters (lower levels of MonoNC, and high levels of MultiNC and BiNC) seen frequently in lymphocytes from lung cancer and COPD patients rather than in those from asthma patients or healthy individuals might be attributed to the high proliferation rate of the affected cells and the inflammatory changes in the microenvironment leading up to the development of chronic pathological condition; blood lymphocytes will travel have to pass for through areas of increased inflammation or oxidative stress (Dai et al. 2017; Anderson et al. 2019). Our results are consistent with research elsewhere which showed that GO NMs possess high anticancer properties (Szmidt et al. 2019). Cultured lymphocytes from lung cancer and COPD patients showed a higher increase in the percentage of BiNC but also the frequency of MNi in BiNC (BiMNi) than those from asthma patients and healthy individuals. Increased levels of BiMNi are a biomarker of cancer susceptibility, and could be used as predictors of cancer in healthy individuals susceptible to DNA damage (El-Zein et al. 2008). Previous research had found that the average NDI value in patients with lung cancer was significantly smaller compared to the negative controls (1.52 vs 2.08, $p<0.001$) (El-Zein et al. 2008) and in colorectal cancer (CRC) patients relative to patients with normal colonoscopy (1.57 vs 1.73). (Ionescu et al. 2011). The group found that the cut-off value that indicated adenomas or carcinomas was 1.5 – that means the lower the NDI value, the higher the likelihood of cancer in this case

However, their values contradict our findings as our NDI values increased with increased concentrations of GO nanomaterials. Some chemicals are known to behave differently such as Oxaliplatin (OXP) where the NDI values in patients with CRC were higher compared to the untreated PBL from healthy negative control individual (1.82 vs 1.73) due to high values of the multinucleated cells (Alotaibi et al. 2017). The results in the CBMN assay are clearly in agreement with the concentration-dependent increases in the cytotoxicity of GO nanomaterial we had established earlier on using the MTT and NRU assays, and in the genotoxicity (DNA damage) studies using the alkaline Comet assay.

Although the CBMN assay is widely used in genetic toxicology studies (İpek et al. 2017), it showed some limitations during the course of our experiments. First, it was rather time-consuming and could lead to increased human error and inter-laboratory discrepancies which makes it unsuitable for field studies where rapid results are required (Radack et al. 1995; Fenech et al. 2003). Secondly, the spindle inhibitor cytochalasin B even though it is used in a low concentration that should not induce significant damage may act in synergy or additive with the treatment chemical inducing more DNA damage or affecting proliferation rates of the lymphocytes (Albertini et al. 2000). Also, a long culture time is an important factor which could lead to overestimation of MNi frequencies, probably due to delayed cell division in the already injured cells. The significant differences in cytogenetic responses in blood lymphocytes from patients vs. those from healthy individuals could be associated with confounding factors of age and smoking history.

5. CONCLUSION

In conclusion, our results are based on GO NMs exposed lymphocytes that were chosen as surrogate cells for somatic cells. If GO NMs are pharmaceutically formulated as nanocarriers in drug delivery to target lung cancer cells and COPD, our results suggest that they could potentially cause DNA damage to healthy cells of COPD and lung patients. Peripheral blood leukocytes from healthy individuals, assumed to be immunocompetent, showed various levels of cytotoxicity, genotoxicity (DNA damage), and chromosome aberrations *in vitro* is a source of concern to public health especially (workplace exposure) and in the paradigm shift into drug delivery applications after the nanomaterials have completed their job at the cancer target sites. The data obtained in our study further complements existing literature on cytotoxicity and genotoxicity of the various types of GO NMs. These results are clear indications of the need for future comprehensive genotoxicity studies of GO (15-20 sheets) both *in vivo* and *in vitro* to develop safer nanomaterials. It is crucial to have a better understanding of the mechanism GO NMs induce DNA damage at the molecular level and to clarify conflicting genotoxicity data available on different types and sizes of GO (Liu et al. 2013; Wu et al. 2015).

iJETRM
International Journal of Engineering Technology Research & Management
(IJETRM)
https://ijetrm.com/

ACKNOWLEDGEMENTS

The authors are grateful to the Nurses at Professor Badie Jacob's Respiratory Clinic, Bradford Royal Infirmary (BRI) and to Dr Abid Aziz Respiratory Consultant at St Luke's Hospital, Bradford, West Yorkshire, UK for the provision of blood samples from lung cancer, asthma, and COPD patients. Dr Emmanuel Eni Amadi acknowledges the Leverhulme Trade Charities Trust, London for the PhD bursary; and to Mr Stuart Fox – the SEM and TEM operator; and Dr Alex Surtees and Dr Mohammed Isreb for training on DLS and ZP in the Analytical Chemistry Lab, Centre for Chemical and Structural Analysis and Institute of Cancer Therapeutics (ICT), University of Bradford.

Conflict of Interests

The authors declare no conflict of interest.

REFERENCES

Albertini, R. J., Anderson, D., Douglas, G. R., Hagmar, L., Hemminki, K., Merlo, F., Natarajan, A. T., Norppa, H., Shuker, D. E. G., Tice, R., Waters, M. D. and Aitio, A. (2000) IPCS guidelines for the monitoring of genotoxic effects of carcinogens in humans. International Programme on Chemical Safety. *Mutation Research-Reviews in Mutation Research* 463 (2), 111-172.

Amadi, E. E. (2019). Effects of Graphene Oxide in vitro on DNA Damage in Human Whole Blood and Peripheral Blood Lymphocytes from Healthy Individuals and Pulmonary Disease Patients: Asthma, COPD, and Lung Cancer [Doctoral dissertation, University of Bradford, UK]. BradScholars. Available at: https://bradscholars.brad.ac.uk/handle/10454/18685

Anderson, D., Najafzadeh, M., Scally, A., Jacob, B., Griffith, J., Chaha, R., Linforth, R., Soussaline, M. and Soussaline, F. (2019) Using a Modified Lymphocyte Genome Sensitivity (LGS) test or TumorScan test to detect cancer at an early stage in each individual. *FASEB Bioadv* 1 (1), 32-39.

Aslantürk, Ö. S. (2017) In Vitro Cytotoxicity and Cell Viability Assays: Principles, Advantages, and Disadvantages. *IntechOpen*.

Azqueta, A. and Dusinska, M. (2015) The use of the comet assay for the evaluation of the genotoxicity of nanomaterials. *Frontiers in Genetics* 6.

Barbero, F., Russo, L., Vitali, M., Piella, J., Salvo, I., Borrajo, M. L., Busquets-Fité, M., Grandori, R., Bastús, N. G., Casals, E. and Puntes, V. (2017) Formation of the Protein Corona: The Interface between Nanoparticles and the Immune System. *Seminars in Immunology* 34, 52-60.

Ben-Ze'ev, A. and Raz, A. (1981) Multinucleation and inhibition of cytokinesis in suspended cells: reversal upon reattachment to a substrate. *Cell* 26 (1 Pt 1), 107-15.

Bhattacharjee, S. (2016) DLS and zeta potential – What they are and what they are not? *Journal of Controlled Release* 235, 337-351.

Bignold, L. P. (2009) Mechanisms of clastogen-induced chromosomal aberrations: A critical review and description of a model based on failures of tethering of DNA strand ends to strand-breaking enzymes. *Mutation Research-Reviews in Mutation Research* 681 (2), 271-298.

Böyum, A. (1968) Separation of leukocytes from blood and bone marrow. Introduction. *Scand J Clin Lab Invest Suppl.* 97 (7).

Clogston, J. D. and Patri, A. K. (2011) Zeta potential measurement. *Methods Mol Biol* 697, 63-70.

Dai, J., Yang, P., Cox, A. and Jiang, G. (2017) Lung cancer and chronic obstructive pulmonary disease: From a clinical perspective. *Oncotarget* 8 (11), 18513.

Daniels, T. R., Delgado, T., Helguera, G. and Penichet, M. L. (2006) The transferrin receptor part II: Targeted delivery of therapeutic agents into cancer cells. *Clinical Immunology* 121 (2), 159-176.

Dinauer, N., Balthasar, S., Weber, C., Kreuter, J., Langer, K. and von Briesen, H. (2005) Selective targeting of antibody-conjugated nanoparticles to leukemic cells and primary T-lymphocytes. *Biomaterials* 26 (29), 5898-5906.

Ding, Z., Zhang, Z., Ma, H. and Chen, Y. (2014) In vitro hemocompatibility and toxic mechanism of graphene oxide on human peripheral blood T lymphocytes and serum albumin. *ACS applied materials & interfaces* 6 (22), 19797-19807.

iJETRM
International Journal of Engineering Technology Research & Management
(IJETRM)
https://ijetrm.com/

El-Zein, R. A., Fenech, M., Lopez, M. S., Spitz, M. R. and Etzel, C. J. (2008) Cytokinesis-Blocked Micronucleus Cytome Assay Biomarkers Identify Lung Cancer Cases Amongst Smokers. *Cancer Epidemiol Biomarkers Prev.* 17 (5), 1111-119.

Fenech, M. (2002) Chromosomal biomarkers of genomic instability relevant to cancer. *Drug Discovery Today* 7 (Generic), 1128-1137.

Fenech, M. (2007) Cytokinesis-block Micronucleus Cytome Assay. *Nature Protocols* 2 (5), 1084-1104.

Fenech, M., Bonassi, S., Turner, J., Lando, C., Ceppi, M., Chang, W. P., Holland, N., Kirsch-Volders, M., Zeiger, E., Bigatti, M. P., Bolognesi, C., Cao, J., De Luca, G., Di Giorgio, M., Ferguson, L. R., Fucic, A., Lima, O. G., Hadjidekova, V. V., Hrelia, P., Jaworska, A., Joksic, G., Krishnaja, A. P., Lee, T.-K., Martelli, A., McKay, M. J., Migliore, L., Mirkova, E., Müller, W.-U., Odagiri, Y., Orsiere, T., Scarfì, M. R., Silva, M. J., Sofuni, T., Suralles, J., Trenta, G., Vorobtsova, I., Vral, A. and Zijno, A. (2003) Intra- and inter-laboratory variation in the scoring of micronuclei and nucleoplasmic bridges in binucleated human lymphocytes: Results of an international slide-scoring exercise by the HUMN project. *Mut.Res.-Genetic Toxicology and Environmental Mutagenesis* 534 (1), 45-64.

Filipe, V., Hawe, A. and Jiskoot, W. (2010) Critical Evaluation of Nanoparticle Tracking Analysis (NTA) by NanoSight for the Measurement of Nanoparticles and Protein Aggregates. *Pharmaceutical Research* 27 (5), 796-810.

Gerashchenko, B. I. (2017) On scoring cytokinetic and binucleated cells. *Cytometry A* 91 (7), 655-656.

Hansen, J. and Bross, P. (2010) A cellular viability assay to monitor drug toxicity. *Methods Mol Biol.* 648, 303-11.

Heshmati, M., Hajibabae, S. and Barikrow, N. (2018) Genotoxicity and Cytotoxicity Assessment of Graphene Oxide Nanosheets on HT29 Cells. *Journal of Kermanshah University of Medical Sciences* 22 (1).

Hondow, N., Brydson, R., Wang, P., Holton, M. D., Brown, M. R., Rees, P., Summers, H. D. and Brown, A. (2012) Quantitative characterization of nanoparticle agglomeration within biological media. *Journal of Nanoparticle Research* 14 (7), 1-15.

Ionescu, M. E., Ciocirlan, M., Becheanu, G., Nicolaie, T., Ditescu, C., Teiusanu, A. G., Gologan, S. I., Arbanas, T. and Diculescu, M. M. (2011) Nuclear Division Index may Predict Neoplastic Colorectal Lesions. *Maedica (Buchar)* 6 (3), 173-178.

Karbaschi, M. and Cooke, M. S. (2014) Novel method for the high-throughput processing of slides for the comet assay. *Scientific reports* 4, 7200.

Kim, J., Cote, L. J. and Huang, J. (2012) Two Dimensional Soft material: new faces of Graphene Oxide. *Accounts of chemical research* 45 (8), 1356-1364.

Kirsch-Volders, M. and Fenech, M. (2001) Inclusion of micronuclei in non-divided mononuclear lymphocytes and necrosis/apoptosis may provide a more comprehensive cytokinesis block micronucleus assay for biomonitoring purposes. *Mutagenesis* 16 (1), 51-58.

Liao, K.-H., Lin, Y.-S., Macosko, C. W. and Haynes, C. L. (2011) Cytotoxicity of graphene oxide and graphene in human erythrocytes and skin fibroblasts. *ACS applied materials & interfaces* 3 (7), 2607-2615.

Liu, J., Cui, L. and Losic, D. (2013)
Graphene and graphene oxide as new nanocarriers for drug delivery applications. *Acta biomaterialia* 9 (12), 9243-9257.

Ma, N., Zhang, P., Zhang, B., Liu, J., Li, Z. and Luan, Y. (2015) Green fabricated reduced graphene oxide: evaluation of its application as nano-carrier for pH-sensitive drug delivery. *International Journal of Pharmaceutics* 496 (2), 984-992.

Mittal, S., Sharma, P. K., Tiwari, R., Rayavarapu, R. G., Shankar, J., Chauhan, L. K. S. and Pandey, A. K. (2017) Impaired lysosomal activity mediated autophagic flux disruption by graphite carbon nanofibers induce apoptosis in human lung epithelial cells through oxidative stress and energetic impairment. *Particle and fibre toxicology* 14 (1), 15-25.

Mohamadi, S. and Hamidi, M. (2017) The new nanocarriers based on graphene and graphene oxide for drug delivery applications. *Nanostructures for Drug Delivery: Micro and Nano Technologies.* Online: 107-147.

Monteiro-Riviere, N. A. and Inman, A. O. (2006) Challenges for assessing carbon nanomaterial toxicity to the skin. *Carbon* 44 (6), 1070-1078.

iJETRM
International Journal of Engineering Technology Research & Management
(IJETRM)
https://ijetrm.com/

Mossman, T. (1983a) Rapid colorimetric assay for cellular growth and survival: application to proliferation and cytotoxicity assays. *Journal of Immunological Methods* 65, 55-63.

Mossman, T. (1983b) Rapid colorimetric assay for cellular growth and survival: Application to proliferation and cytotoxicity assays. *Journal of Immunological Methods* 65 (1-2), 55-63.

Nasongkla, N., Shuai, X., Ai, H., Weinberg, B. D., Pink, J., Boothman, D. A. and Gao, J. (2004) cRGD-functionalized polymer micelles for targeted doxorubicin delivery. *Angewandte Chemie - International Edition* 43 (46), 6323-6327.

OECD (2016) Test No. 489: In Vivo Mammalian Alkaline Comet Assay. *https://www.oecd-ilibrary.org/docserver/9789264264885-en.pdf?expires=1543337897&id=id&accname=guest&checksum=6DC18CD4BF2F11016194FC0BB182F0D5* Accessed 27th Nov 2018

Orlow, I., Park, B. J., Mujumdar, U., Patel, H., P., S.-L., Clas, B., R., D., Flores, R., Bains, M., Rizk, N., Dominguez, G., Jani, J., Berwick, M., Begg, C., Kris, M. and Rusch, V. (2015) DNA Damage and Repair Capacity in Lung Cancer Patients: Prediction of Multiple Primary Tumors. *J Clin Oncol.* 26 (21), 3560-3566.

Ou, L., Song, B., Liang, H., Liu, J., Feng, X., Deng, B., Sun, T. and Shao, L. (2016) Toxicity of graphene-family nanoparticles: a general review of the origins and mechanisms. *Particle and fibre toxicology* 13 (1), 57.

Parveen, S., Misra, R. and Sahoo, S. (2012) Nanoparticles: a boon to drug delivery, therapeutics, diagnostics and imaging. *Nanomedicine* 8 (2), 147-166.

Podrimaj-Bytyqi, A., Borovečki, A., Selimi, Q., Manxhuka-Kerliu, S., Gashi, G. and Elezaj, I. R. (2018) The frequencies of micronuclei, nucleoplasmic bridges and nuclear buds as biomarkers of genomic instability in patients with urothelial cell carcinoma. *Scientific Reports* 8 (1), 17873.

Powers, K. W., Brown, S. C., Krishna, V. B., Wasdo, S. C., Moudgil, B. M. and Roberts, S. M. (2006) Research strategies for safety evaluation of nanomaterials. Part VI. Characterization of nanoscale particles for toxicological evaluation. *Toxicological sciences : an official journal of the Society of Toxicology* 90 (2), 296-303.

Radack, K. L., Pinney, S. M. and Livingston, G. K. (1995) Sources of variability in the human lymphocyte micronucleus assay: a population-based study. *Environ Mol Mutagen* 26 (1), 26-36.

Rebuttini, V., Fazio, E., Santangelo, S., Neri, F., Caputo, G., Martin, C., Brousse, T., Favier , F. and Pinna, N. (2015) Chemical Modification of Graphene Oxide through Diazonium Chemistry and Its Influence on the Structure–Property Relationships of Graphene Oxide–Iron Oxide Nanocomposites. *Chemistry – A European Journal* 21 (35), 12465-12474.

Repetto, G., del Peso, A. and Zurita, J. L. (2008) Neutral red uptake assay for the estimation of cell viability/cytotoxicity. *Nature Protocols* 3 (7), 1125-1131.

Sasidharan, A., Panchakarla, L. S., Sadanandan, A. R., Ashokan, A., Chandran, P., Girish, C. M., Menon, D., Nair, S. V., Rao, C. N. R. and Koyakutty, M. (2012) Hemocompatibility and macrophage response of pristine and functionalized graphene. *Small (Weinheim an der Bergstrasse, Germany)* 8 (8), 1251-1263.

Seshadri, D. R. and Ramamurthi, A. (2018) Nanotherapeutics to Modulate the Compromised Micro-Environment for Lung Cancers and Chronic Obstructive Pulmonary Disease. *Frontiers in pharmacology* 9, 759.

Singh, S. K., Singh, M. K., Kulkarni, P. P., Sonkar, V. K., Grácio, J. J. A. and Dash, D. (2012) Amine-Modified Graphene: Thrombo-Protective Safer Alternative to Graphene Oxide for Biomedical Applications. *ACS Nano* 6 (3), 2731-2740.

Singh, S. K., Singh, M. K., Nayak, M. K., Kumari, S., Shrivastava, S., Grácio, J. J. A. and Dash, D. (2011) Thrombus Inducing Property of Atomically Thin Graphene Oxide Sheets. *ACS Nano* 5 (6), 4987-4996.

Song, J., Wang, X. and Chang, C.-T. (2014) Preparation and Characterization of Graphene Oxide. *Journal of Nanomaterials* 2014, 1-6.

STEMCELL Technologies (2017) *Lymphoprep Density Gradient Medium for the Isolation of mononuclear cells.* 2017. Online: STEMCELL Technologies Canada Inc. *https://cdn.stemcell.com/media/files/pis/29283-PIS_1_3_0.pdf?_ga=2.11894386.777538854.1552913845-1383156917.1552913845*

iJETRM
International Journal of Engineering Technology Research & Management
(IJETRM)
https://ijetrm.com/

Stephenson, A. P., Schneider, J. A., Nelson, B. C., Atha, D. H., Jain, A., Soliman, K. F. A., Aschner, M., Mazzio, E. and Renee Reams, R. (2013) Manganese-induced oxidative DNA damage in neuronal SH-SY5Y cells: Attenuation of thymine base lesions by glutathione and N-acetylcysteine. *Toxicology Letters* 218 (3), 299-307.

Stetefeld, J., McKenna, S. A. and Patel, T. R. (2016) Dynamic light scattering: a practical guide and applications in biomedical sciences. *Biophys Rev* 8 (4), 409-427.

Stone, V., Johnston, H. and Schins, R. (2009) Development of in vitro systems for nanotoxicology: methodological considerations. *Crit Rev Toxicol.* 39 (7), 613-26.

Stéfani, D., Paula, A. J., Vaz, B. G., Silva, R. A., Andrade, N. F., Justo, G. Z., Ferreira, C. V., Filho, A. G. S., Eberlin, M. N. and Alves, O. L. (2011) Structural and proactive safety aspects of oxidation debris from multiwalled carbon nanotubes. *Journal of Hazardous Materials* 189 (1), 391-396.

Sun, X., Liu, Z., Welsher, K., Robinson, J. T., Goodwin, A., Zaric, S. and Dai, H. (2008) Nano-graphene oxide for cellular imaging and drug delivery. *Nano Res.* 1 (3), 203-212.

Szmidt, M., Stankiewicz, A., UrbaAska, K., Jaworski, S., Kutwin, M., Wierzbicki, M., Grodzik, M., BurzyAska, B., Gora, M., Chwalibog, A. and Sawosz, E. (2019) Graphene oxide down-regulates genes of the oxidative phosphorylation complexes in a glioblastoma. *BMC Molecular Biology* 20 (1), 1-9.

Tice, R. R., Agurell, A., D., Burlinson, B., Hartmann, A., Kobayashi, H., Miyamae, Y., Rojas, E., Ryu, J.-C. and Sasaki, Y. F. (2000) Single Cell Gel/Comet Assay: Guidlines for In Vitro and In Vivo Genetic Toxicology Testing. *Environmental and Molecular Mutagenesis* 35, 206-221.

U.S. National Library of Medicine (2019) *Lung Cancer.* Online: *https://ghr.nlm.nih.gov/condition/lung-cancer* Accessed 20 Mar 2019.

Vargas-Rondon, Villegas, V. E. and Rondon-Lagos, M. (2018) The Role of Chromosomal Instability in Cancer and Therapeutic Responses. *Cancers (Based)* 10 (4).

Wang, K., Ruan, J., Song, H., Zhang, J., Wo, Y., Guo, S. and Cui, D. (2011a) Biocompatibility of Graphene Oxide. *Nanoscale Research Letters* 6 (1), 1-8.

Wang, Y., Wang, J., Li, J., Li, Z. and Lin, Y. (2011b) Graphene and graphene oxide: biofunctionalization and applications in biotechnology. *Trends in Biotechnology* 29 (5), 205-212.

Wills, J. W., Summers, H. D., Hondow, N., Sooresh, A., Meissner, K. E., White, P. A., Rees, P., Brown, A. and Doak, S. H. (2017) Characterizing Nanoparticles in Biological Matrices: Tipping Points in Agglomeration State and Cellular Delivery In Vitro. *ACS Nano* 11 (12), 11986-12000.

Winey, M., Meehl, J. B., O'Toole, E. T. and Giddings, J. T. H. (2014) Conventional transmission electron microscopy. *Molecular biology of the cell* 25 (3), 319-323.

Wu, S.-Y., An, S. S. A. and Hulme, J. (2015) Current applications of graphene oxide in nanomedicine. *International journal of nanomedicine* 10 Spec Iss, 9-24.

Yang, K., Zhang, S., Zhang, G., Sun, X., Lee, S.-T. and Liu, Z. (2010) Graphene in mice: Ultrahigh in vivo tumor uptake and efficient photothermal therapy. *Nano Letters* 10 (9), 3318-3323.

Zhao, X., Yang, L., Li, X., Jia, X., Liu, L., Zeng, J., Guo, J. and Liu, P. (2015) Functionalized graphene oxide nanoparticles for cancer cell-specific delivery of antitumor drug. *Bioconjugate chemistry* 26 (1), 128-136.

İpek, E., Ermiş, E., Uysal, H., Kızılet, H., Demirelli, S., Yıldırım, E., Ünver, S., Demir, B. and Kızılet, N. (2017) The relationship of micronucleus frequency and nuclear division index with coronary artery disease SYNTAX and Gensini scores. *Anatol J Cardiol* 17 (6), 483-489.

iJETRM
International Journal of Engineering Technology Research & Management
(IJETRM)
https://ijetrm.com/

FIGURES

Figure 1. Characterisation of GO NM,15-20 sheets. Micrographs: SEM: (A) = 50x Mag.; Scale Bar: 1.0 mm; TEM: (B): 20,000x mag.; Scale Bar: 2.0 µm; (C): 20,000 mag.; Scale Bar: 2.0 µm, respectively.

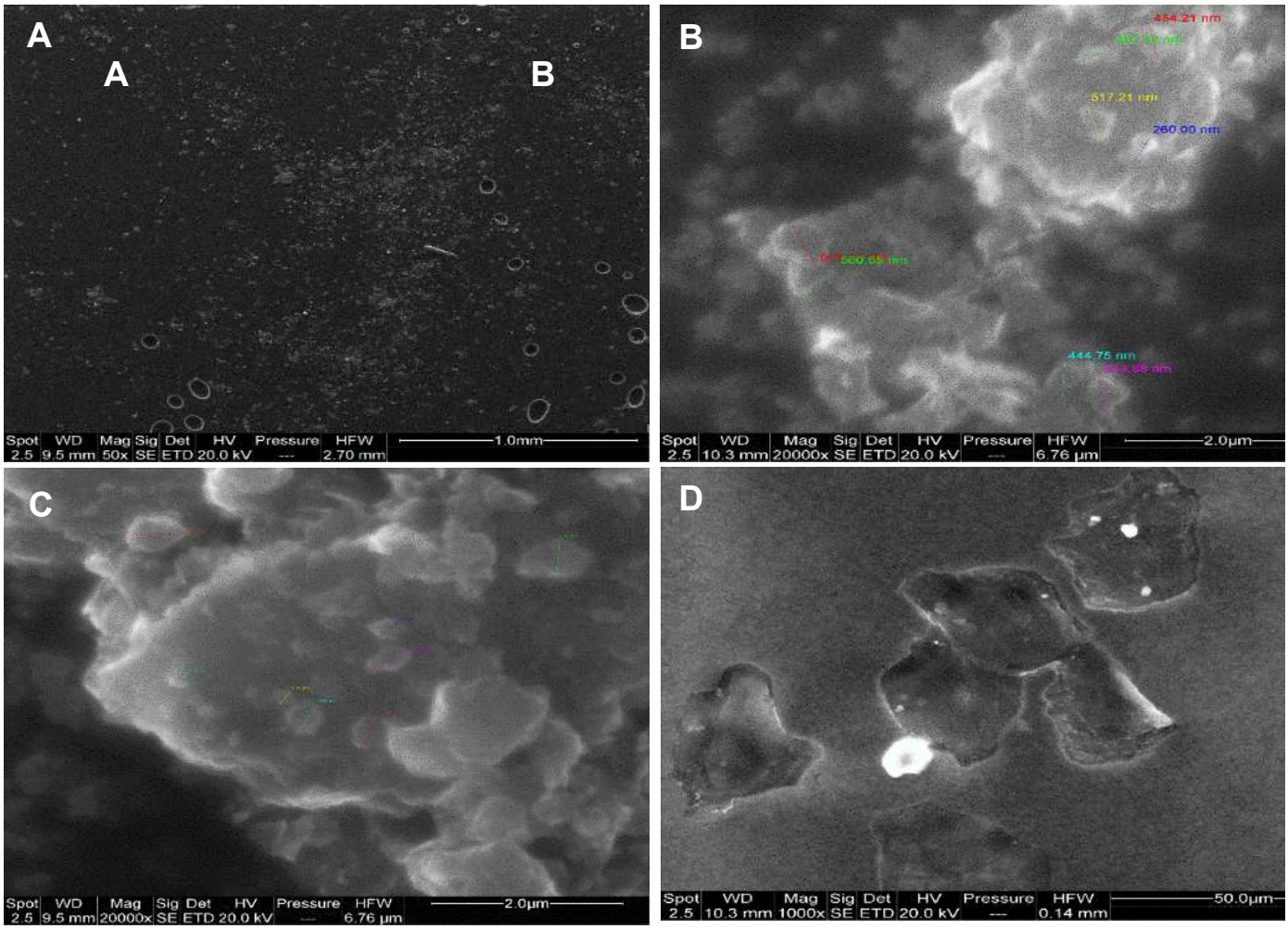

iJETRM
International Journal of Engineering Technology Research & Management
(IJETRM)
https://ijetrm.com/

Figure 2. Cytotoxicity of GO (15-20 sheets) in peripheral human lymphocytes after 24 h treatment with different concentrations of GO (0.1, 0.2, 0.5 and 1 µg/ml). The mitochondrial activities were assessed with NRU and MTT assays. The percentage (%) of cell survival of treated lymphocytes was compared with untreated lymphocytes (0 µg/ml: negative control = 100%) in healthy control individuals and pulmonary asthma, COPD, and lung cancer patients. The values represent the mean ± SEM of three independent experiments (n=3). * $p < 0.05$; ** $p < 0.01$; *** $p < 0.001$; ns = not statistically different. Bars indicate standard errors.

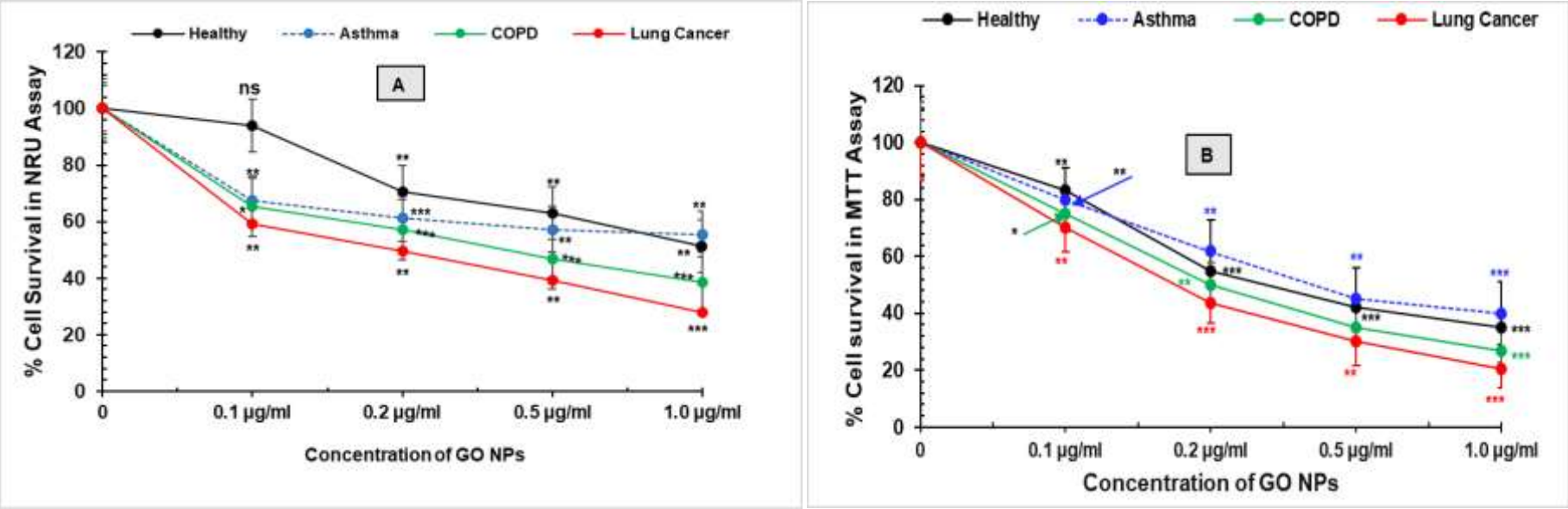

iJETRM
International Journal of Engineering Technology Research & Management
(IJETRM)
https://ijetrm.com/

Figure 3. Using histograms to compare the DNA damaging effects of graphene oxid (15-20 sheets) at concentrations of 0.1, 0.2, 0.5, and 1.0 µg/ml and H_2O_2 (100 µM) in human white blood cells from healthy individuals and asthma, COPD, and lung cancer patients. Cells were treated for 30 min before being subjected to the Comet assay. DNA damage was expressed as: **(A)** Olive tail moment (OTM); and (**B)** the percentage of DNA in the comet tail (% Tail DNA). Statistical significance was rated as $p < 0.05$; where * denotes $p < 0.05$; ** $p < 0.01$; *** $p < 0.001$; and ns = not significant; based on 20 x independent Comet assay experiments per treatment group, and a total of 80 Comet assays (n = 80).

iJETRM
International Journal of Engineering Technology Research & Management
(IJETRM)
https://ijetrm.com/

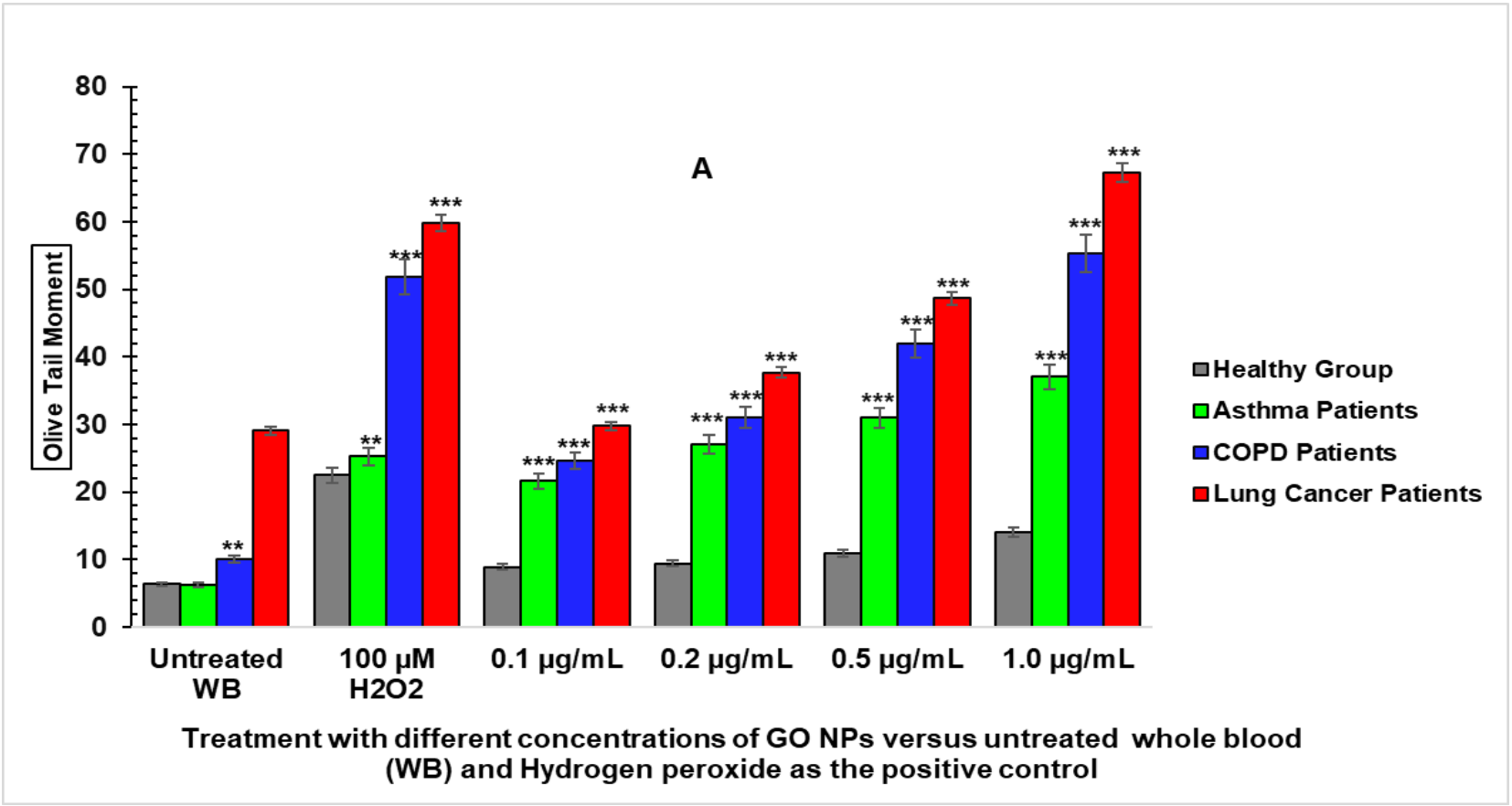

Treatment with different concentrations of GO NPs versus untreated whole blood (WB) and Hydrogen peroxide as the positive control

iJETRM
International Journal of Engineering Technology Research & Management
(IJETRM)
https://ijetrm.com/

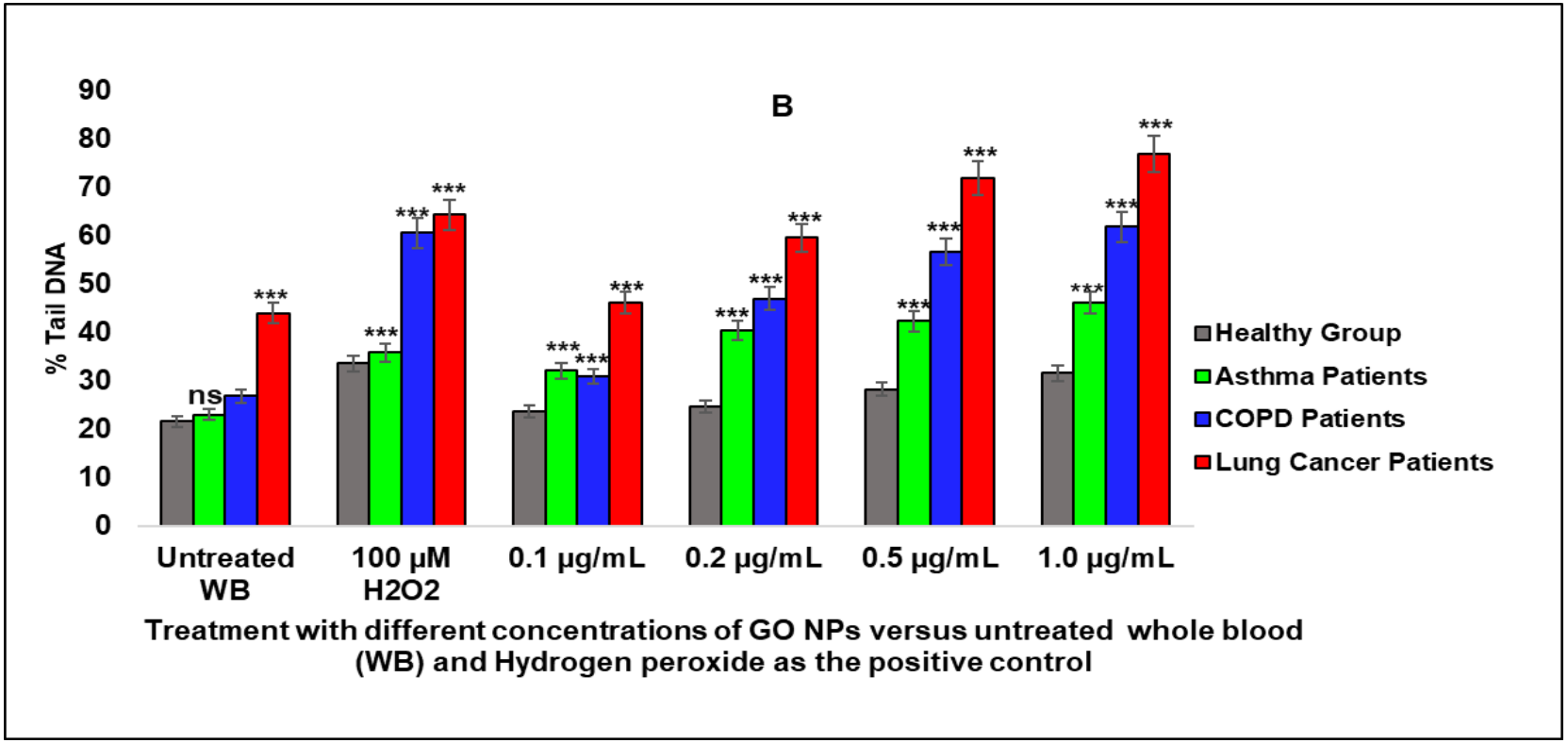

Treatment with different concentrations of GO NPs versus untreated whole blood (WB) and Hydrogen peroxide as the positive control

Table 1. Demographic data of recruited healthy control individuals with no history of smoking and no medical history of severe disease. Note: Samples from donors highlighted in grey were used for cytotoxicity studies.

SN	Code	Age (years)	Sex	Ethnicity	Smoking History	Medical History
1	10335	39	M	Caucasian	None	None
2	10329	39	F	Caucasian	None	None
3	10331	69	M	Caucasian	None	None
4	JW 27-8-15 (Box 91)	40	M	Caucasian	None	None
5	23-24 (Box 84)	44	F	Caucasian	None	None
6	No-35-36	56	F	Caucasian	None	None
7	17-06-15 MA	47	M	Caucasian	None	None
8	MS 23-06-15	39	M	Caucasian	None	None
9	10588	32	F	Asian	None	None
10	10-12-18	47	M	Caucasian	None	None
11	AM	45	F	Caucasian	None	None
12	WJ	47	M	Caucasian	None	None
13	AN	43	M	Caucasian	None	None
14	HC	56	M	Caucasian	None	None
15	JH	24	M	Caucasian	None	None
16	TA	42	F	Caucasian	None	None
17	PN	39	F	Caucasian	None	None
18	AH	48	M	Caucasian	None	None
19	NA	50	M	Caucasian	None	None
20	EW	46	F	Caucasian	None	None

Table 2. Demographic data of recruited patients diagnosed with asthma. Note: Sections in grey were used for cytotoxicity studies. Note: Samples from donors highlighted in grey were used for cytotoxicity studies.

SN	Code	Age (years)	Sex	Ethnicity	Smoking History	Medical History
1	27-10-15 R	45	M	Caucasian	Smoker, 3-5/day	None
2	21-10-15 R	32	F	Caucasian	Non-smoker	None
3	13-3-17 R4 0339423	31	F	Asian	Non-smoker	None
4	13-3-17 R2 0505001	61	M	Caucasian	Smoker; 40/day; 30/year	Asthma & COPD
5	13-3-17 R3 0538130	54	F	Caucasian	Smoker; 15-20/ day	Asthma & COPD
6	R 21-10-15	32	F	Caucasian	Non -Smoker	NA
7	RAE 0144596	47	F	Caucasian	Not recorded	None
8	9/3/17 R2 RAE 1317552	54	F	Caucasian	Past Smoker	None
9	R4 13-3-17	64	M	Caucasian	Non - Smoker	None
10	24/2/17 RAE 0797968	38	F	Caucasian	Not recorded	None
11	9-3-17	49	M	Caucasian	Smoker; 3/day	None
12	03-12-18	64	F	Asian	Non - Smoker	None
13	6-12-18	46	F	Asian	Non - Smoker	None
14	1182462; 4500698388	61	M	Caucasian	Non - Smoker	None
15	N/A	65	M	Caucasian	Non-Smoker	None
16	N/A	58	F	Caucasian	Non-Smoker	None
17	N/A	60	M	Caucasian	Non-Smoker	None
18	0809845	26	F	Caucasian	Non-Smoker	None
19	PU	64	F	Asian	Non-Smoker	None
20	TA	46	F	Asian	Non-Smoker	None

Table 3. Demographic data of recruited patients diagnosed with COPD. Note: Sections in grey were used for cytotoxicity studies. Note: Samples from donors highlighted in grey were used for cytotoxicity studies.

SN	Code	Age (years)	Sex	Ethnicity	Smoking History	Medical History
1	5-8-15 R2	52	M	Caucasian	Smoker; 20/day	None
2	09-06-15 R	65	F	Caucasian	Smoker; 5-10/day	None
3	13-3-17 R2 0505001	61	M	Caucasian	Smoker; 40/day; 30/year	Asthma & COPD
4	13-3-17 R3 0538130	54	F	Caucasian	Smoker; 15-20/day	Asthma & COPD
5	13-3-17 R1 1308631	56	F	Caucasian	Past Smoker	None
6	R 09-06-15	55	M	Caucasian	Smoker; 20-80/day	None
7	R2 05-08-15	64	M	Caucasian	Smoker	None
8	R1 27-2-17; RAE 0255865	64	M	Caucasian	Smoker; 20/day	None
9	R3 27-2-17 DJ1	54	F	Caucasian	Smoker; 6-8/day	None
10	R3 28-2-17	69	M	Caucasian	Smoker	None
11	R1 2-3-17 RAE 1165577	64	M	Caucasian	Smoker; 20/day	None
12	R2 2-3-17 RAE 0716425	70	F	Caucasian	Smoker; 15-20/day for 20 yrs	Severe COPD/ recurrent chest infection
13	9/3/17 R1 RAE 0292614	49	M	Asian	Smoker; 20/day; Cannabis; pop usually	COPD; Schizophrenia
14	6-12-18	54	F	Caucasian	Past Smoker; Tobacco	None
15	3340032	57	M	Caucasian	Smoker	None
16	367885	59	M	Caucasian	Smoker; 30/day	None
17	4360497856	57	M	Caucasian	Smoker	None
18	CX	58	M	Caucasian	Past Smoker	None
19	QX	54	F	Caucasian	Past Smoker/ tobacco	None
20	0290072	57	M	Caucasian	Smoker; 30/day; alcohol	None

Table 4. Demographic data of recruited patients diagnosed with lung cancer. Note: Sections in grey were used for cytotoxicity studies. Note: Samples from donors highlighted in grey were used for cytotoxicity studies.

SN	Code	Age (years)	Sex	Ethnicity	Smoking History	Medical History
1	5-8-15 R3	64	M	Caucasian	Smoker; 8/ day	None
2	29-7-15 R	62	M	Caucasian	Smoker; 10-15/day	None
3	05-08-15 R	62	F	Asian	Non -Smoker	None
4	06-08-15 R2	74	M	Caucasian	10-15/day	None
5	05-08-15 R1	60	F	Asian	Non - Smoker	None
6	R1 7-12-2016	64	M	Caucasian	Smoker	None
7	R2 7-12-2016	77	F	Caucasian	Smoker	None
8	12-1-17	64	M	Caucasian	Smoker	Lung nodule
9	13-12-18	55	F	Asian	Past Smoker	None
10	0795624	65	M	Caucasian	Smoker; 30 pack/ year	None
11	0564145	72	F	Caucasian	Smoker	None
12	0290072	57	M	Caucasian	Smoker; 30/day	Pulmonary fibrosis; COPD
13	N/A	60	F	Caucasian	Past Smoker	None
14	N/A	50	M	Caucasian	Past Smoker	None
15	N/A	65	M	Asian	Past Smoker	None
16	N/A	61	F	Caucasian	Past Smoker	None
17	N/A	68	M	Caucasian	Past Smoker	None
18	ZA	55	F	Asian	Past Smoker	None
19	4360497856	57	M	Caucasian	Smoker; 30/day	None
20	0795624	65	M	Caucasian	30 pack/ year	None

Table 5. Characterization of GO NM in DLS showing the agglomeration states (Z-average): hydrodynamic diameter (d.nm), polydispersity index (PdI); surface charge (Zeta potential) in aqueous solution. Average particle size = 760 ± 31 nm; PdI = 0.87 ± 0.05 and average Zeta potential = -23.9 ± 2 mV. TEM and SEM analyses showed particle sizes ranging from 364 ± 29 to 448 ± 60 nm per 15-20 layers, while the size of each layer ranged from 18 to 30 nm.

DLS analysis			**SEM and TEM analyses**			
Zeta Potential (mV)	**Polydispersity Index (PdI)**	**Agglomeration State: Z-average hydrodynamic diameter (nm) of 15-20 layers**	**Particle distance (nm) of 15-20 layers of GO dispersed in an aqueous solution**			
			10 µg/ml	**20 µg/ml**	**50 µg/ml**	**100 µg/ml**
		760 ± 31	**364 ± 29**	**418 ± 54**	**384 ± 67**	**448 ± 60**
-23 ± 2	0.87 ± 0.05					
Average single layer (nm)		**38-51**	**18-24**	**21-28**	**19-26**	**22-30**

Table 6. Mean values of various biomarkers of cytogenetic damage in PBL from the healthy control group, asthma group, COPD group and lung cancer group after treatment with graphene oxide (GO) using the CBMN assay (n = 5). DNA damage events were scored binucleated cells (BiNC) and mononucleated cells (MonoNC). MNi induction was statistically significant at 1 µg/ml ($p < 0.05$). Abbreviations: MMC = mitomycin C, MultiNC = multinucleated cells, NDI = nuclear division index, MNi = micronuclei, NPBs = nucleoplasmic bridges and BUDs = nuclear buds.

Healthy Control Group		Mean %MonoNC	Mean %BiNC	Mean %MultiNC	Mean NDI	Mean BiMNi	Mean BiNPBs	Mean BiNBUDs	Mean MonoMNi
NC	**0 µg/ml**	38.12±1.10	61.16±1.11	1.44±0.20	1.63±0.01	1.80±0.66	0.00±0.00	0.00±0.00	0.40±0.24
MMC (PC)	**0.4 µM**	18.4±0.70 ***	79.56±0.58 ***	4.08±0.34 ***	1.84±0.01 ***	2.8±0.58 ***	0.80±0.49 ***	0.80±0.37 ***	1.20±0.20 ***
GO (µg/ml)	**0.1**	33.40±0.41 ***	65.72±0.42 ***	1.76±0.20 ***	1.69±0.02 ***	0.80±0.37 ***	0.20±0.20 ***	0.00±0.00 ns	0.20±0.20 ***
	0.2	29.76±0.39 ***	69.08±0.40 ***	2.32±0.15 ***	1.71±0.00 ***	1.00±0.32 ***	0.20±0.20 ***	0.20±0.20 ***	0.80±0.37 ***
	0.5	27.52±1.02 ***	71.12±0.99 ***	2.72±0.15 ***	1.74±0.01 ***	3.00±0.71 ***	0.00±0.00 ns	0.20±0.20 ***	1.60±0.24 ***
	1	24.52±0.63 ***	73.52±0.26 ***	4.47±0.41 ***	1.79±0.00 ***	2.80±0.66 ***	0.60±0.24 ***	0.40±0.24 ***	2.60±0.93 ***
Asthma Group									
NC	**0 µg/ml**	35.20±0.81	63.84±0.88	1.92±0.27	1.66±0.01	2.40±0.98	0.00±0.00	0.40±0.24	1.00±0.32
MMC (PC)	**0.4 µM**	23.08±0.34 ***	75.36±0.25 ***	3.12±0.34 ***	1.70±0.08 ***	6.20±0.86 ***	0.80±0.37 ***	0.60±0.40 ***	1.60±0.68 ***
GO (µg/ml)	**0.1**	34.28±0.85 ***	64.76±086 ***	1.92±0.08 ns	1.67±0.01 ***	1.50±0.26 ***	0.00±0.00 ns	0.50±0.26 ***	0.50±0.26 ***
	0.2	30.96±0.32 ***	67.80±0.32 ***	2.48±0.15 ***	1.80±0.66 ***	1.80±0.66 ***	0.60±0.40 ***	0.40±0.24 ns	0.80±0.37 ***
	0.5	27.08±0.45	70.72±0.46 ***	2.80±0.13 ***	1.74±0.60 ***	5.20±0.80 ***	0.60±0.24 ***	1.60±0.24 ***	1.80±0.80 ***
	1	25.16±0.79 ***	72.24±0.72 ***	5.20±0.44 ***	1.77±0.01 ***	5.80±1.24 ***	1.20±0.58 ***	1.40±0.60 ***	5.20±0.97 ***
COPD Group									
NC	**0 µg/ml**	33.12±0.55	65.72±0.52	2.32±0.15	1.69±0.01	3.80±0.80	0.00±0.00	0.20±0.20	2.60±0.40
MMC (PC)	**0.4 µM**	22.52±1.29 ***	75.52±1.26 ***	3.92±0.32 ***	1.79±0.01 ***	6.80±1.28 ***	0.80±0.37 ***	0.80±0.37 ***	3.40±1.03 ***
GO (µg/ml)	**0.1**	31.84±0.31 ***	66.84±0.25 ***	2.64±0.16 ***	1.69±0.00 ns	3.20±0.58 ***	0.00±0.00 ns	0.20±0.20 ns	1.40±0.40 ***
	0.2	29.00±0.40 ***	69.92±0.43 ***	2.16±0.10 ***	1.72±0.00 ***	5.60±1.03 ***	0.80±0.49 ***	0.80±0.20 ***	3.00±0.89 ***
	0.5	24.60±0.45 ***	72.88±0.34 ***	4.40±0.31 ***	1.77±0.01 ***	5.80±1.46 ***	0.40±0.24 ***	0.80±0.37 ***	3.00±0.84 ***
	1	21.52±0.55 ***	75.84±0.66 ***	5.28±0.74 ***	1.81±0.01 ***	6.00±0.45 ***	0.60±0.24 ***	1.40±0.40 ***	3.20±1.11 ***
Lung Cancer Group									
NC	**0 µg/ml**	32.24±1.80	66.16±1.64	3.20±0.42	1.69±0.02	3.40±0.51	2.00±0.63	0.00±0.00	2.80±0.66
MMC (PC)	**0.4 µM**	19.44±0.81 ***	77.56±0.66 ***	6.00±0.36 ***	1.84±0.01 ***	8.0±0.45 ***	1.00±0.40 ***	0.40±0.40 ***	5.80±0.37 ***
GO (µg/ml)	**0.1**	29.56±0.44 ***	68.84±0.46 ***	3.20±0.13 ns	1.72±0.00 ***	4.40±1.14 ***	0.20±0.20 ***	0.60±0.24 ***	3.60±1.37 ***
	0.2	25.24±0.99 ***	72.56±0.95 ***	4.40±1.01 ***	1.77±0.01 ***	5.80±0.37 ***	1.00±0.32 ***	1.20±0.20 ***	4.80±0.66 ***
	0.5	22.72±0.92 ***	74.56±0.84 ***	5.44±0.30 ***	1.80±0.01 ***	7.40±0.51 ***	0.40±0.24 ***	0.60±0.40 ***	6.20±0.66 ***
	1	15.56±1.31 ***	80.04±1.26 ***	8.80±0.68 ***	1.89±0.01 ***	9.40±0.51 ***	1.00±0.45 ***	1.00±0.32 ***	7.40±0.51 ***

Table 7. Confounding factors within the blood donors.

Group	Present/past smoker	Non-smoker	Age rage (Years)	Frequency	Percentage
Healthy	0	20 (100%)	20-29	1	5%
			30-39	5	25%
			40-49	10	50%`
			50-59	3	15%
			60-69	1	5%
Asthma	5 (25%)	13 (65%)	20-29	1	5%
			30-39	4	20%
			40-49	5	25%
			50-59	3	15%
			60-69	7	35%
COPD	20 (100%)	0	40-49	1	5%
			50-59	12	60%
			60-69	6	30%
			70-79	1	5%
Lung cancer	18 (90%)	2 (10%)	50-59	5	25%
			60-69	12	60%
			70-79	3	15%